

Journal of Neuroendocrinology**Sex- and sub region-dependent modulation of arcuate kisspeptin neurons by vasopressin and vasoactive intestinal peptide**

Journal:	<i>Journal of Neuroendocrinology</i>
Manuscript ID	JNE-18-0113-OA.R1
Manuscript Type:	Original Article
Date Submitted by the Author:	n/a
Complete List of Authors:	Schafer, Danielle; University of Otago, Centre for Neuroendocrinology and Department of Physiology Kane, Grace; University of Otago, Centre for Neuroendocrinology and Department of Physiology Colledge, William; University of Cambridge, Physiology, Development and Neuroscience Piet, Richard; Otago School of Medical Sciences, Physiology Herbison, Allan; University of Otago, Centre for Neuroendocrinology and Department of Physiology
Keywords:	Kisspeptin, GnRH, Neurokinins, Vasopressin, calcium, sex differences



1
2
3 **1 Revised**
4
5
6

7 **3 Sex- and sub region-dependent modulation of arcuate kisspeptin neurons by**
8 **4 vasopressin and vasoactive intestinal peptide**
9

10
11
12 **6 Danielle Schafer¹, Grace Kane¹, William H. Colledge², Richard Piet¹,**
13 **7 Allan E. Herbison¹**
14

15
16
17 **9 ¹Centre for Neuroendocrinology and Department of Physiology, School of**
18 **10 Biomedical Sciences, University of Otago, Dunedin 9054, New Zealand, and**
19 **11 ²Reproductive Physiology Group, Department of Physiology, Development and**
20 **12 Neuroscience, University of Cambridge, Cambridge CB2 3EG, United Kingdom.**
21
22

23
24
25 **14 *Short title:* Neuropeptide modulation of arcuate kisspeptin neurons**
26
27
28
29
30
31
32

33 **20 Correspondence to:**

34 **21 Allan E. Herbison**

35 **22 Centre for Neuroendocrinology and Department of Physiology, Otago School of**
36 **23 Medical Sciences, University of Otago, Dunedin, New Zealand 9054**

37 **24 Tel +64 3 479 7312**

38 **25 Email: allan.herbison@otago.ac.nz**
39
40
41
42
43

44 **30 Key words: GCAMP, kisspeptin, neurokinin B, sex differences, vasoactive intestinal**
45 **31 peptide, vasopressin**
46
47
48
49
50
51
52
53
54
55
56
57
58
59
60

Abstract

A population of kisspeptin neurons located in the hypothalamic arcuate nucleus (ARN) very likely represent the gonadotrophin-releasing hormone pulse generator responsible for driving pulsatile luteinizing hormone secretion in mammals. As such, it has become important to understand the neural inputs that modulate the activity of ARN kisspeptin (ARN^{KISS}) neurons. Using a transgenic GCaMP6 mouse model allowing the intracellular calcium levels ($i[Ca^{2+}]$) of individual ARN^{KISS} neurons to be assessed simultaneously, we examined whether the circadian neuropeptides vasoactive intestinal peptide (VIP) and arginine vasopressin (AVP) modulated the activity of ARN^{KISS} neurons directly. To validate this methodology, we initially evaluated the effects of neurokinin B (NKB) on $i[Ca^{2+}]$ in kisspeptin neurons residing within the rostral, middle and caudal ARN subregions of adult male and female mice. All experiments were undertaken in the presence of tetrodotoxin and ionotropic amino acid antagonists. NKB was found to evoke an abrupt increase in $i[Ca^{2+}]$ in 95-100% of kisspeptin neurons throughout the ARN of both sexes. In marked contrast, both VIP and AVP were found to primarily activate kisspeptin neurons located in the caudal ARN of female mice. Whereas 58 and 59% of caudal ARN kisspeptin neurons responded to AVP and VIP, respectively, in female mice, only 0-8% of kisspeptin neurons located in other ARN subregions responded in females and 0-12% of cells in any subregion in males ($p < 0.05$). These observations demonstrate unexpected sex differences and marked heterogeneity in functional neuropeptide receptor expression amongst ARN^{KISS} neurons organized on a rostro-caudal basis. The functional significance of this unexpected influence of VIP and AVP on ARN^{KISS} neurons remains to be established.

57 Introduction

58 The pulsatile release of luteinizing hormone (LH) is critical for fertility. Adult males
59 exhibit an LH pulse approximately every 3h while females show variable LH pulse
60 rates ranging from a pulse every hour in the follicular phase to one every 3h in the
61 luteal phase of the cycle (1). However, a variety of internal and external factors can
62 drive LH pulse frequency outside this normal range to suppress fertility. For example,
63 the high LH pulse frequency of females with polycystic ovary syndrome and slow
64 pulsatility observed in hypothalamic amenorrhea are often associated with infertility
65 (2-4).

66 Studies examining a range of mammalian species over recent years have indicated
67 that kisspeptin neurons co-expressing neurokinin B and dynorphin (KNDy neurons)
68 located in the hypothalamic arcuate nucleus are responsible for generating the
69 pulsatile pattern of gonadotropin-releasing hormone (GnRH) release that drives
70 pulsatile LH secretion (1, 5). As such, the arcuate nucleus KNDy or kisspeptin
71 (ARN^{KISS}) neurons have become a focal point for investigators wanting to understand
72 how different physiological and pathophysiological factors influence LH pulse
73 frequency (1, 6, 7).

74 Although the definition and role of circadian inputs to the preoptic population of
75 kisspeptin neurons has received much attention (8, 9), no information exists
76 regarding the potential circadian regulation of the ARN^{KISS} neurons. Studies in
77 humans have identified sleep-wake variations in LH pulse frequency (10-12) raising
78 the possibility that some form of circadian input may also be directed at the ARN^{KISS}
79 neurons. To begin to investigate this possibility, we have examined whether ARN^{KISS}
80 neurons in the mouse express functional receptors for arginine vasopressin (AVP)
81 and vasoactive intestinal peptide (VIP), the two major neuropeptidergic outputs from
82 the suprachiasmatic nucleus (SCN). **Studies in rats and mice have identified receptors
83 for both of these neuropeptides in the arcuate nucleus (13-15) and SCN neurons are
84 known to project to and modulate the activity of ARN neurons in the rat (16, 17).
85 However, we note that many neural populations expressing VIP and AVP are also
86 found outside the SCN and may conceivably have a role in regulating LH secretion.**

87

1
2
3 88 To examine the potential effects of AVP and VIP, we have established a transgenic
4
5 89 GCaMP6 calcium imaging approach that enables the effects of neurotransmitters on
6
7 90 adult ARN^{KISS} neurons to be assessed in the acute brain slice. To ensure that we
8
9 91 measure direct effects of these neuropeptides on kisspeptin neurons, intracellular
10
11 92 calcium concentrations ($[Ca^{2+}]_i$) were assessed in the presence of amino acid receptor
12
13 93 antagonists and tetrodotoxin (TTX).
14
15

16 95 **Materials and Methods**

17 96 *Experimental animals*

18
19 97 Mice were generated by crossing *Kiss1-Cre*^{+/-} (18) and homozygous floxed GCaMP6f
20
21 98 (Ai95(RCL-GCaMP6f)-D)(19) lines to generate mixed background *129S6Sv/Ev*
22
23 99 *C57BL6 Kiss1-Cre::GCaMP6f-lox-STOP-lox (Kiss1::GCaMP6)* mice. Mice were group-
24
25 100 housed under conditions of controlled temperature (22±2°C) and lighting (12-hour
26
27 101 light/12-hour dark cycle (lights on at 6:00h and off at 18:00h) with *ad libitum* access
28
29 102 to food and water. The University of Otago Animal Ethics Committee approved all
30
31 103 animal experimental protocols.
32

33 104 34 105 *Immunohistochemistry*

35 106 Four adult female *Kiss1::GCaMP6f* mice were ovariectomized under Halothane
36
37 107 anesthesia and 3-weeks later anesthetized and perfused through the heart with 4%
38
39 108 paraformaldehyde, phosphate-buffered saline for free-floating dual
40
41 109 immunofluorescence histochemistry as reported previously (20, 21). Mice were
42
43 110 ovariectomized so as to increase the level of kisspeptin peptide in ARN neurons to
44
45 111 improve immunohistochemical detection. Primary antisera raised against GFP
46
47 112 (rabbit 1:5,000, Invitrogen; RRID:AB_221570) and kisspeptin (sheep 1:1,000, AC053
48
49 113 gift of Alain Caraty, Nouzilly, France)(22) were used to increase the GCaMP6 signal
50
51 114 and detect kisspeptin, respectively. Secondary antisera were biotinylated donkey
52
53 115 anti-sheep immunoglobulins (1:200, Jackson ImmunoResearch Labs, PA) followed by
54
55 116 streptavidin-568 (1:200, Molecular Probes), and donkey anti-rabbit-488 (1:200,
56
57 117 Jackson), respectively. Dual-fluorescence images were captured on a NikonA1+

1
2
3 118 inverted confocal microscope. Two sections at each of the rostral, middle and caudal
4
5 119 levels of the ARN were analyzed in each mouse by counting the total number of cells
6
7 120 that expressed GFP (GCaMP6) and/or kisspeptin.

8 121
9 122 *Calcium imaging*

10
11 123 The $i[Ca^{2+}]$ of multiple ARN^{KISS} neurons was monitored simultaneously in acute brain
12
13 124 slices using a methodology previously established for the preoptic kisspeptin
14
15 125 neurons (23). Coronal brain slices (250 μ m-thick) containing the rostral, middle and
16
17 126 caudal regions of the ARN were prepared from adult male and diestrous-stage female
18
19 127 *Kiss1::GCaMP6f* mice between 10:00-11:00h (N=4 for each sex, region and
20
21 128 neuropeptide) and constantly perfused (1mL/min) with 30°C, 95%O₂/5%CO₂
22
23 129 equilibrated, artificial cerebrospinal fluid (aCSF) comprised of (mM) NaCl 120, KCl 3,
24
25 130 NaHCO₃ 26, NaH₂PO₄ 1, CaCl₂ 2.5, MgCl₂ 1.2 and glucose 10. To ensure that only direct
26
27 131 neuropeptide responses were recorded from ARN^{KISS} neurons, the aCSF contained
28
29 132 TTX (0.5 μ M) and the ionotropic GABA_A and glutamate receptor antagonists
30
31 133 picrotoxin (100 μ M), CNQX (10 μ M), and AP5 (40 μ M) at all times (all sourced from
32
33 134 Tocris Biosciences). Slices were placed under an upright Olympus BX51W1
34
35 135 microscope and multiple individual cells in a plane of focus visualized through a 40x
36
37 136 immersion objective using a xenon arc light source (300 W, filtered by a GFP filter
38
39 137 cube (excitation 470-490 nm, Chroma)) and a DG-4 shutter (Sutter Instruments)
40
41 138 providing 100ms duration light at 2Hz. Epifluorescence (495 nm long pass and
42
43 139 emission 500-520 nm) was collected using a Hamamatsu ORCA-ER digital CCD
44
45 140 camera.

46
47 141 The effects of neuropeptides on ARN^{KISS} neuron GCaMP6f fluorescence were assessed
48
49 142 by measuring basal fluorescence over a 4 min period and then adding the test
50
51 143 neuropeptide to the aCSF for a two-min period before switching back to aCSF only.
52
53 144 Regions of interest over individual, non-overlapping, and in-focus fluorescent somata
54
55 145 were selected and analyzed using ImageJ software and custom R scripts. Individual
56
57 146 cells were considered to have responded if they exhibited an increase in fluorescence
58
59 147 during the 2-min test period that was greater than their mean baseline level + 2
60

1
2
3 148 standard deviations (SD) derived from basal recordings. To accommodate for the
4
5 149 gradual decline in fluorescence levels that occurs over the test period, the
6
7 150 fluorescence levels over the first 4-min basal period were divided into the first (b1)
8
9 151 and second (b2) two-minute basal recording periods and an adjusted baseline (F) for
10
11 152 the 2-min stimulation period set at = $b2 - (b1 - b2)$. For visualizing data, values are
12
13 153 presented as relative fluorescence changes using $\frac{\Delta F}{F} = \frac{F_t - F}{F} * 100$ where F is the
14
15 154 adjusted baseline and F_t is the fluorescence measured.

16
17 155 To assess effects of neuropeptides on ARN^{KISS} neuron located at different rostro-
18
19 156 caudal levels of the ARN, four rostral, four middle and four caudal slices from four
20
21 157 separate mice were tested with each neuropeptide. The different rostrocaudal levels
22
23 158 were determined by the distinctive topography of kisspeptin neurons in each area
24
25 159 and the shape of the median eminence (Fig.1). Each slice received only one test.
26
27 160 Results are reported as number of cells examined (n) and numbers of slices or mice
28
29 161 (N). **The effects of neurokinin B (NKB, 50nM), AVP (300nM) and VIP (1 μ M) (Tocris**
30
31 162 **Bioscience) were examined.** Prior studies in the laboratory have shown that these
32
33 163 concentrations are effective in activating the firing of kisspeptin, GnRH and other
34
35 164 neurons in acute brain slices (23-25). Statistical analysis comparing between sexes
36
37 165 and ARN subregions was undertaken with two-way ANOVA and *post-hoc* Tukey tests.

38 166

39 167 **Results**

40 168 *Expression of GCaMP6 in arcuate nucleus kisspeptin neurons*

41 169 The distribution of GCaMP6-expressing cells throughout the rostro-caudal extent of
42
43 170 the ARN in *Kiss1::GCaMP6f* mice (Fig.1A) was identical to that reported for kisspeptin
44
45 171 neurons (21) with the largest numbers of cells detected in the caudal ARN (Table).
46
47 172 Dual-label immunofluorescence demonstrated that 88-95% of GCaMP6 cells
48
49 173 expressed kisspeptin and virtually all (99%) kisspeptin neurons contained GCaMP6
50
51 174 (Fig.1B-D, Table).

52 175

53 176 *GCaMP6 calcium imaging*

1
2
3 177 The GCaMP6 imaging enabled the fluorescence levels of 8-25 ARN^{KISS} neurons to be
4
5 178 evaluated simultaneously in each brain slice. Initial control experiments in slices
6
7 179 from four diestrous female mice showed that 53 of the 54 recorded cells (N=4 slices)
8
9 180 exhibited a stable baseline level of fluorescence that gradually declined over time
10
11 181 (Fig.2). Only one of the 54 cells was found to show spontaneous fluctuations (Fig.2).

12 182

13 183 *NKB activates all kisspeptin neurons in the ARN of males and females*

14 184 To test the validity of this preparation, we first examined the effects of NKB as this
15
16 185 neuropeptide has been reported to have direct stimulatory effects on the firing of
17
18 186 nearly all ARN^{KISS} neurons in male mice (24, 26, 27). Exposure to 50nM NKB was
19
20 187 found to evoke an increase in fluorescence levels in essentially all GCaMP6-
21
22 188 expressing cells located throughout the ARN (Fig.3A-C). Responses could be abrupt
23
24 189 or take over 1 min to occur with baseline levels typically restored to normal within 4-
25
26 190 5 min of the response (Fig.3C). In four diestrous *Kiss1::GCaMP6f* female mice, 37
27
28 191 rostral, 100 middle, and 65 caudal cells were tested in four brain slices from each
29
30 192 region with 100% of cells exhibiting a change in fluorescence signal that was > basal
31
32 193 + 2SD. The same result was found for male mice (N=4) with 28/28 rostral, 75/79
33
34 194 (95%) middle and 84/87 (97%) caudal cells responding to NKB (Fig.3D). **Basal**
35
36 195 **fluorescence signals in males were the same as those observed for females with only**
37
38 196 **occasional evidence of spontaneous calcium transients.** No significant differences
39
40 197 were detected between any regions or sexes ($p > 0.05$, Two-way ANOVA).

41 198

42 199 *VIP activates caudal arcuate kisspeptin neurons in a sexually dimorphic manner.*

43
44 200 The administration of 1 μ M VIP was found to have no effects upon GCaMP6
45
46 201 fluorescence in 35 kisspeptin neurons (N=4) located in the rostral-aspect of the ARN
47
48 202 in female *Kiss1::GCaMP6f* mice (Fig.4A). While the middle ARN (N=4) was similar
49
50 203 with only 2/58 (3%) cells responding, 46/80 (58%) kisspeptin neurons in the caudal
51
52 204 ARN (N=4) were activated by VIP (Fig.4A,B; $p < 0.05$ compared with other subregions,
53
54 205 Two-way ANOVA, post-hoc Tukey's tests). These responses could take up to 2 min to
55
56 206 initiate and typically exhibited a fluctuating profile before returning to baseline up to

1
2
3 207 10 min later (Fig.4B). **Although a relationship between the basal level of fluorescence**
4 **and the magnitude of any response existed, responding cells could not be predicted**
5 **by their basal level of fluorescence.** In male *Kiss1::GCaMP6f* mice, no cells in the
6
7 209 rostral (n=32, N=4) or middle aspects of the ARN (n=71, N=4) responded to VIP with
8
9 210 only 3/57 (6%, N=4) kisspeptin neurons in the caudal stimulated (p<0.05 compared
10
11 211 to females, Two-way ANOVA, post-hoc Tukey's tests; Fig. 4C).
12
13 212

14 213
15 214 *AVP activates caudal arcuate kisspeptin neurons in a sexually dimorphic manner.*

16 215 Exposure to 300nM AVP had minimal effects on fluorescence levels in kisspeptin
17
18 216 neurons located in the rostral (2/34 cell responded, 6%, N=4) and middle (5/66 cells,
19
20 217 8%, N=4) aspects of the ARN but increased intracellular calcium levels in 46 of 78
21
22 218 (59%, N=4) cells located in the caudal ARN (Fig.5A; p<0.05 compared with other
23
24 219 subregions, Two-way ANOVA, post-hoc Tukey's tests). Responses evoked by AVP
25
26 220 were typically immediate upon entry of AVP into the bath but short-lived, sometimes
27
28 221 terminating during the application period (Fig.5B). In male *Kiss1::GCaMP6f* mice, 4-
29
30 222 12% of kisspeptin neurons responded throughout the rostro-caudal extent of the
31
32 223 ARN; 1/24 rostral (4%), 5/67 middle (8%) and 10/81 caudal (12%)(N=4 each,
33
34 224 Fig.5C). The numbers of kisspeptin neurons responding to AVP were significantly
35
36 225 different in the caudal ARN of females compared to other subregions and males
37
38 226 (p<0.05 compared to females, Two-way ANOVA, post-hoc Tukey's tests; Fig. 5C).
39
40 227

41 228 42 229 **Discussion**

43 230
44 231 We report here the unexpected observation that kisspeptin neurons located at
45
46 232 different rostro-caudal locations within the ARN can express different functional
47
48 233 neuropeptide receptors and, further, that this is sexually dimorphic. Whereas all
49
50 234 ARN^{KISS} neurons in both males and females express tachykinin receptors activated by
51
52 235 NKB, the kisspeptin neurons activated by AVP and VIP are located primarily within
53
54 236 the caudal ARN and exhibit a marked female-dominant sex difference. These
55
56 237 observations highlight the functional heterogeneity and striking sexually dimorphic

238 nature of the ARN^{KISS} neuron population and, further, indicate that this may be
239 organized in a rostro-caudal topographic manner.

240

241 The *Kiss1::GCaMP6f* mouse line was found to provide high fidelity targeting of
242 GCaMP6 to the ARN^{KISS} neuron population with essentially 100% of kisspeptin
243 neurons expressing GCaMP6 and these cells representing 88-95% of all GCaMP6
244 neurons located in the ARN. As such, this mouse line provides a good model
245 preparation for examining the direct responses of *ex-vivo* ARN^{KISS} neurons to putative
246 neurotransmitters and neuropeptides. Nevertheless, the approach has caveats,
247 principally being that inhibitory effects of transmitters, or receptor activation that
248 does not directly or indirectly modulate $i[Ca^{2+}]$, will not be revealed. Thus, false
249 negatives may occur but positive responses will be indicative of the presence of
250 cognate receptors for the transmitter examined.

251

252 Prior electrophysiological brain slice studies have shown that 90-100% of ARN^{KISS}
253 neurons are activated by NKB or tachykinin receptor agonists in male mice (24, 26,
254 27). In good agreement, we find that essentially 100% of ARN^{KISS} neurons in intact
255 male mice respond directly to NKB with elevated $i[Ca^{2+}]$ and now extend this to
256 demonstrate that this is also the case in diestrous female mice. Prior studies using
257 dual-label *in situ* hybridization have reported that 75-100% of ARN^{KISS} neurons
258 located in the middle aspects of the ARN express *Tacr3* transcripts in female mice (27,
259 28). By targeting recordings to the rostral, middle and caudal aspects of the ARN we
260 are able to demonstrate remarkable consistency in the functional expression of NKB-
261 activated receptors by ARN^{KISS} neurons in both males and females. **As a sub-
262 population of ARN^{KISS} neurons will be the GnRH pulse generator, these observations
263 are in good agreement with *in vivo* data showing that intracerebroventricular
264 administration of senktide, an NK3R agonist, activates LH secretion in both intact
265 male and diestrous-stage female mice (29).**

266

267 In striking contrast to the effects of NKB, both AVP and VIP exerted subregion- and
268 sex-dependent effects on ARN^{KISS} neuron $i[Ca^{2+}]$. Whereas 58% of caudal ARN^{KISS}

1
2
3 269 neurons responded to VIP in females only 6% were activated in male, and essentially
4
5 270 no cells were stimulated in the rostral or middle regions of the ARN in either sex.
6
7 271 Similarly, 58% of caudal ARN^{KISS} neurons were activated by AVP compared with only
8
9 272 4 -12% of neurons in other regions or in males. This indicates that female caudal
10
11 273 ARN^{KISS} neurons preferentially express functional receptors for VIP and AVP.
12 274 **Although not addressed in this study, it is possible that changes in ARN^{KISS} neuron**
13
14 275 **sensitivity to AVP and VIP may occur with postnatal development or across the**
15
16 276 **estrous cycle in females.**

17 277
18
19 278 Similar numbers of caudal ARN^{KISS} neurons are activated by AVP and VIP in female
20
21 279 but they evoke very different profiles of changing $i[Ca^{2+}]$. The molecular identities of
22
23 280 the receptors activated are not known although VIP at 1 μ M concentrations would be
24
25 281 expected to activate both type 1 (VPAC1) and type 2 (VPAC2) VIP receptors in
26
27 282 addition to the pituitary adenylate cyclase-activating peptide (PACAP) receptor (30).
28
29 283 Recent studies have shown that PACAP neurons located in the preammillary
30
31 284 nucleus project to ARN^{KISS} neurons and can directly activate a sub-population of
32
33 285 caudal ARN neurons in female mice (31). **Hence, it is possible that PACAP is the**
34
35 286 **endogenous ligand for VIP receptors expressed by ARN^{KISS} neurons.** Recent
36
37 287 transcriptome-based cell sorting strategies failed to identify any AVP or VIP/PACAP
38
39 288 receptor transcripts in pools of ARN^{KISS} neurons from young female or mixed
40
41 289 male/female mice (32, 33). Given the sex-dependent and highly regionalised nature
42
43 290 of AVP and VIP receptor expression revealed here, future transcriptomic studies of
44
45 291 ARN^{KISS} neuron will need to take potential subregion and sex differences into
46
47 292 consideration.

48 293
49 294 The sex- and region-specific nature of AVP and VIP effects identified here would not
50
51 295 support the concept of a generalized direct circadian regulation of ARN^{KISS} neurons
52
53 296 by these neuropeptides. Studies have found day-night differences in LH pulse
54
55 297 frequency in both human males and females (10-12) although their dependence on
56
57 298 circadian cues, as opposed to environmental influences such as sleep and stress, has

1
2
3 299 been challenged (34). Further, while studies in rodents have identified circadian-like
4
5 300 changes in LH secretion in peripubertal females, it has remained unclear whether this
6
7 301 was related to pulse or surge modes of LH secretion (35). Hence, it is possible that
8
9 302 there is no direct or substantial circadian modulation of the different ARN^{KISS} neuron
10
11 303 sub-populations. Instead, VIP/PACAP and AVP inputs to ARN^{KISS} neurons may
12
13 304 originate from neural populations located outside the suprachiasmatic nucleus, as
14
15 305 has recently been demonstrated for PACAP neurons of the premammillary nucleus
16
17 306 (31). Interestingly, preliminary viral retrograde tracing data indicate that
18
19 307 vasopressin neurons in the supraoptic nucleus project to ARN^{KISS} neurons (Yeo &
20
21 308 Colledge, unpublished).

309

22 310 The function of neuropeptidergic inputs directed at caudal ARN^{KISS} neurons in the
23
24 311 female can only be speculated upon at present. Sex differences in ARN^{KISS} morphology
25
26 312 and function have been documented (20, 36) but the extent to which this depends on
27
28 313 sexually differentiated inputs is unknown. Further, the functions of AVP/VIP-
29
30 314 sensitive ARN^{KISS} neurons are unknown and may even be unrelated to the regulation
31
32 315 of GnRH neurons. Indeed, tract tracing studies have shown that caudal ARN^{KISS}
33
34 316 neurons project to multiple limbic brain region in the mouse (37). On the other hand,
35
36 317 recent optogenetic studies have indicated that the ARN^{KISS} neuron pulse generator
37
38 318 may be located in the middle-caudal aspects of the nucleus (21) although no further
39
40 319 features or markers of this population have been identified as yet. One intriguing
41
42 320 speculation is that SCN inputs to ARN^{KISS} neurons may modulate the LH surge.
43
44 321 Although there is little evidence for the ARN to be involved in the timing of the LH
45
46 322 surge (38), recent studies have suggested that the ARN^{KISS} neurons may be involved
47
48 323 in regulating the amplitude of the LH surge (39, 40), potentially through direct
49
50 324 projections to preoptic area kisspeptin neurons (41).

325

51 326 In summary, these studies reveal marked sex- and subregion-specific effects of two
52
53 327 neuropeptides on ARN^{KISS} neurons. These observations reinforce the concept of
54
55 328 functional heterogeneity amongst the ARN^{KISS} neuron population. Alongside other
56
57 329 evidence (21, 37), it seems that this heterogeneity may, in part, be organized on a

1
2
3 330 rostral-caudal basis within the ARN of the mouse. In contrast, we find that the
4
5 331 response of ARN^{KISS} neurons to NKB is extremely uniform impacting upon essentially
6
7 332 all kisspeptin neurons throughout the nucleus in both males and females. The
8
9 333 functional relevance of this heterogeneity with respect to pulse generation as well as
10
11 334 other functions of the ARN^{KISS} neuron population awaits elucidation. More
12
13 335 specifically, the surprising observation of sexually dimorphic and region-specific AVP
14
15 336 and VIP signaling within the ARN^{KISS} neuron population raises intriguing questions as
16
17 337 to the roles of these neuropeptides within the ARN.

18 338

19 339

20 340

21 341 **Acknowledgements**

22 342 This work was supported by University of Otago Health Science Division Masters
23 343 Scholarship (DS) and the New Zealand Health Research Council. Author
24 344 Contributions: DS designed and performed calcium imaging studies, GK performed
25 345 immunohistochemistry studies, WH provided essential reagents, RP designed
26 346 research and analysed data, AH designed research, analysed data and co-wrote the
27 347 manuscript alongside the other authors.

348 **References**

- 349 1. Herbison AE. The gonadotropin-releasing hormone pulse generator. *Endocrinology*.
350 2018; *Endocrinology*, en.2018-00653.
- 351 2. Jayasena CN, Franks S. The management of patients with polycystic ovary syndrome.
352 *Nature reviews Endocrinology*. 2014; 10: 624-636.
- 353 3. Burt Solorzano CM, Beller JP, Abshire MY, Collins JS, McCartney CR, Marshall JC.
354 Neuroendocrine dysfunction in polycystic ovary syndrome. *Steroids*. 2012; 77: 332-
355 337.
- 356 4. Fourman LT, Fazeli PK. Neuroendocrine causes of amenorrhea--an update. *J Clin*
357 *Endocrinol Metab*. 2015; 100: 812-824.
- 358 5. Goodman RL, Okhura S, Okamura H, Coolen LM, Lehman MN. KNDy hypothesis
359 for generation of GnRH pulses; evidence from sheep and goats. In: Herbison AE, Plant
360 TM, eds. *The GnRH neuron and its control*. Hoboken, NJ, USA: John Wiley and Sons
361 Ltd 2018: 289-324.
- 362 6. Herbison AE. Control of puberty onset and fertility by gonadotropin-releasing
363 hormone neurons. *Nature reviews Endocrinology*. 2016; 12: 452-466.
- 364 7. Yeo SH, Colledge WH. The Role of Kiss1 Neurons As Integrators of Endocrine,
365 Metabolic, and Environmental Factors in the Hypothalamic-Pituitary-Gonadal Axis.
366 *Frontiers in endocrinology*. 2018; 9: 188.
- 367 8. Kriegsfeld LJ. Circadian regulation of kisspeptin in female reproductive functioning.
368 *Adv Exp Med Biol*. 2013; 784: 385-410.
- 369 9. Simonneaux V, Bahougne T. A Multi-Oscillatory Circadian System Times Female
370 Reproduction. *Frontiers in endocrinology*. 2015; 6: 157.
- 371 10. Spratt DI, O'Dea LS, Schoenfeld D, Butler J, Rao PN, Crowley WF, Jr.
372 Neuroendocrine-gonadal axis in men: frequent sampling of LH, FSH, and testosterone.
373 *Am J Physiol*. 1988; 254: E658-666.
- 374 11. Boyar R, Finkelstein J, Roffwarg H, Kapen S, Weitzman E, Hellman L.
375 Synchronization of augmented luteinizing hormone secretion with sleep during
376 puberty. *N Engl J Med*. 1972; 287: 582-586.
- 377 12. Collins JS, Beller JP, Burt Solorzano C, Patrie JT, Chang RJ, Marshall JC, McCartney
378 CR. Blunted day-night changes in luteinizing hormone pulse frequency in girls with
379 obesity: the potential role of hyperandrogenemia. *J Clin Endocrinol Metab*. 2014; 99:
380 2887-2896.
- 381 13. Lukas M, Bredewold R, Neumann ID, Veenema AH. Maternal separation interferes
382 with developmental changes in brain vasopressin and oxytocin receptor binding in
383 male rats. *Neuropharmacology*. 2010; 58: 78-87.
- 384 14. Mounien L, Bizet P, Boutelet I, Gourcerol G, Fournier A, Vaudry H, Jegou S. Pituitary
385 adenylate cyclase-activating polypeptide directly modulates the activity of
386 proopiomelanocortin neurons in the rat arcuate nucleus. *Neuroscience*. 2006; 143:
387 155-163.
- 388 15. Ronnekleiv OK, Fang Y, Zhang C, Nestor CC, Mao P, Kelly MJ. Research resource:
389 Gene profiling of G protein-coupled receptors in the arcuate nucleus of the female.
390 *Mol Endocrinol*. 2014; 28: 1362-1380.

16. Yi CX, van der Vliet J, Dai J, Yin G, Ru L, Buijs RM. Ventromedial arcuate nucleus communicates peripheral metabolic information to the suprachiasmatic nucleus. *Endocrinology*. 2006; 147: 283-294.
17. Guzman-Ruiz M, Saderi N, Cazarez-Marquez F, Guerrero-Vargas NN, Basualdo MC, Acosta-Galvan G, Buijs RM. The suprachiasmatic nucleus changes the daily activity of the arcuate nucleus alpha-MSH neurons in male rats. *Endocrinology*. 2014; 155: 525-535.
18. Yeo SH, Kyle V, Morris PG, Jackman S, Sinnott-Smith LC, Schacker M, Chen C, Colledge WH. Visualisation of Kiss1 neurone distribution using a Kiss1-CRE transgenic mouse. *J Neuroendocrinol*. 2016; 28.
19. Madisen L, Garner AR, Shimaoka D, Chuong AS, Klapoetke NC, Li L, van der Bourg A, Niino Y, Egolf L, Monetti C, Gu H, Mills M, Cheng A, Tasic B, Nguyen TN, Sunkin SM, Benucci A, Nagy A, Miyawaki A, Helmchen F, Empson RM, Knopfel T, Boyden ES, Reid RC, Carandini M, Zeng H. Transgenic mice for intersectional targeting of neural sensors and effectors with high specificity and performance. *Neuron*. 2015; 85: 942-958.
20. Han SY, McLennan T, Czielesky K, Herbison AE. Selective optogenetic activation of arcuate kisspeptin neurons generates pulsatile luteinizing hormone secretion. *Proc Natl Acad Sci U S A*. 2015; 112: 13109-13114.
21. Clarkson J, Han SY, Piet R, McLennan T, Kane GM, Ng J, Porteous RW, Kim JS, Colledge WH, Iremonger KJ, Herbison AE. Definition of the hypothalamic GnRH pulse generator in mice. *Proc Natl Acad Sci U S A*. 2017; 114: E10216-E10223.
22. Franceschini I, Yeo SH, Beltramo M, Desroziers E, Okamura H, Herbison AE, Caraty A. Immunohistochemical evidence for the presence of various kisspeptin isoforms in the Mammalian brain. *J Neuroendocrinol*. 2013; 25: 839-851.
23. Piet R, Fraissenon A, Boehm U, Herbison AE. Estrogen permits vasopressin signaling in preoptic kisspeptin neurons in the female mouse. *J Neurosci*. 2015; 35: 6881-6892.
24. de Croft S, Boehm U, Herbison AE. Neurokinin B activates arcuate kisspeptin neurons through multiple tachykinin receptors in the male mouse. *Endocrinology*. 2013; 154: 2750-2760.
25. Piet R, Dunckley H, Lee K, Herbison AE. Vasoactive intestinal peptide excites GnRH neurons in male and female mice. *Endocrinology*. 2016: en20161399.
26. Ruka KA, Burger LL, Moenter SM. Regulation of arcuate neurons coexpressing kisspeptin, neurokinin B, and dynorphin by modulators of neurokinin 3 and kappa-opioid receptors in adult male mice. *Endocrinology*. 2013; 154: 2761-2771.
27. Navarro VM, Gottsch ML, Wu M, Garcia-Galiano D, Hobbs SJ, Bosch MA, Pinilla L, Clifton DK, Dearth A, Ronnekleiv OK, Braun RE, Palmiter RD, Tena-Sempere M, Alreja M, Steiner RA. Regulation of NKB pathways and their roles in the control of Kiss1 neurons in the arcuate nucleus of the male mouse. *Endocrinology*. 2011; 152: 4265-4275.
28. Navarro VM, Gottsch ML, Chavkin C, Okamura H, Clifton DK, Steiner RA. Regulation of gonadotropin-releasing hormone secretion by kisspeptin/dynorphin/neurokinin B neurons in the arcuate nucleus of the mouse. *J Neurosci*. 2009; 29: 11859-11866.
29. Navarro VM, Bosch MA, Leon S, Simavli S, True C, Pinilla L, Carroll RS, Seminara SB, Tena-Sempere M, Ronnekleiv OK, Kaiser UB. The integrated hypothalamic

- 1
2
3 437 tachykinin-kisspeptin system as a central coordinator for reproduction. *Endocrinology*.
4 438 2015; 156: 627-637.
- 5 439 30. Harmar AJ, Fahrenkrug J, Gozes I, Laburthe M, May V, Pisegna JR, Vaudry D,
6 440 Vaudry H, Waschek JA, Said SI. Pharmacology and functions of receptors for
7 441 vasoactive intestinal peptide and pituitary adenylate cyclase-activating polypeptide:
8 442 IUPHAR review 1. *Br J Pharmacol*. 2012; 166: 4-17.
- 9 443 31. Ross RA, Leon S, Madara JC, Schafer D, Fergani C, Maguire CA, Verstegen AM,
10 444 Brengle E, Kong D, Herbison AE, Kaiser UB, Lowell BB, Navarro VM. PACAP
11 445 neurons in the ventral premammillary nucleus regulate reproductive function in the
12 446 female mouse. *eLife*. 2018; 7.
- 13 447 32. Chen R, Wu X, Jiang L, Zhang Y. Single-Cell RNA-Seq Reveals Hypothalamic Cell
14 448 Diversity. *Cell reports*. 2017; 18: 3227-3241.
- 15 449 33. Campbell JN, Macosko EZ, Fenselau H, Pers TH, Lyubetskaya A, Tenen D, Goldman
16 450 M, Verstegen AM, Resch JM, McCarroll SA, Rosen ED, Lowell BB, Tsai LT. A
17 451 molecular census of arcuate hypothalamus and median eminence cell types. *Nat*
18 452 *Neurosci*. 2017; 20: 484-496.
- 19 453 34. Klingman KM, Marsh EE, Klerman EB, Anderson EJ, Hall JE. Absence of circadian
20 454 rhythms of gonadotropin secretion in women. *J Clin Endocrinol Metab*. 2011; 96:
21 455 1456-1461.
- 22 456 35. Urbanski HF, Ojeda SR. The juvenile-peripubertal transition period in the female rat:
23 457 establishment of a diurnal pattern of pulsatile luteinizing hormone secretion.
24 458 *Endocrinology*. 1985; 117: 644-649.
- 25 459 36. Desroziers E, Mikkelsen JD, Duittoz A, Franceschini I. Kisspeptin-immunoreactivity
26 460 changes in a sex- and hypothalamic-region-specific manner across rat postnatal
27 461 development. *J Neuroendocrinol*. 2012; 24: 1154-1165.
- 28 462 37. Yeo SH, Herbison AE. Projections of arcuate nucleus and rostral periventricular
29 463 kisspeptin neurons in the adult female mouse brain. *Endocrinology*. 2011; 152: 2387-
30 464 2399.
- 31 465 38. Herbison AE. Physiology of the adult GnRH neuronal network. In: Plant TM, Zeleznik
32 466 AJ, eds. *Knobil and Neill's Physiology of Reproduction*. 4th ed: Academic Press 2015:
33 467 399-467.
- 34 468 39. Mittelman-Smith MA, Krajewski-Hall SJ, McMullen NT, Rance NE. Ablation of
35 469 KNDy Neurons Results in Hypogonadotropic Hypogonadism and Amplifies the
36 470 Steroid-Induced LH Surge in Female Rats. *Endocrinology*. 2016; 157: 2015-2027.
- 37 471 40. Helena CV, Toporikova N, Kalil B, Stathopoulos AM, Pogrebna VV, Carolino RO,
38 472 Anselmo-Franci JA, Bertram R. KNDy Neurons Modulate the Magnitude of the
39 473 Steroid-Induced Luteinizing Hormone Surges in Ovariectomized Rats.
40 474 *Endocrinology*. 2015; 156: 4200-4213.
- 41 475 41. Qiu J, Nestor CC, Zhang C, Padilla SL, Palmiter RD, Kelly MJ, Ronnekleiv OK. High-
42 476 frequency stimulation-induced peptide release synchronizes arcuate kisspeptin
43 477 neurons and excites GnRH neurons. *eLife*. 2016; 5: e16246.
- 44 478

1
2
3 **479 Figure legends**
4

5 480

6
7 **481 Figure 1.** Distribution of GCaMP6 in arcuate nucleus (ARN). **A.** Images from the same
8 adult female mouse showing the GFP-immunofluorescence (GCaMP6) in the rostral,
9 482 middle and caudal levels of the ARN. **B-D,** confocal images showing dual fluorescence
10 483 for GFP- (B) and kisspeptin- (C) immunofluorescence, and with the overlapping
11 484 signals represented in D.
12
13 485
14
15 486

16
17 **487 Figure 2.** *Baseline GCaMP6 fluorescence levels in arcuate kisspeptin neurons.* **A.** Raw
18 fluorescence levels of eight ARN kisspeptin neurons located in a middle arcuate
19 488 nucleus brain slice over 12 min. **B.** Higher resolution change in fluorescence levels of
20 489 5 of these cells showing the one cell (cell 3) that exhibited spontaneous fluctuations.
21
22 490
23
24 491

25
26 **492 Figure 3.** *NKB activates essentially all kisspeptin neurons in both male and female mice.*
27 **A.** Single frame photograph of GCaMP6 fluorescence in the middle ARN of a slice being
28 493 imaged. The five cells shown in C are labelled. **B.** Raw fluorescence recordings from
29 494 21 kisspeptin neurons in that brain slice showing their response to a 2-min
30 application of 50nM NKB (grey bar) in the presence of TTX and amino acid receptor
31 495 antagonists. **C.** Higher resolution change in fluorescence levels from the five cells
32 496 depicted in A. Colors are the same as in B. **D.** Histogram showing the percentage of
33 497 kisspeptin neurons in the rostral, middle and caudal aspects of the ARN that
34 498 responded to NKB in male and female mice (N=4, each).
35
36 499
37
38 500
39
40 501

41
42 **502 Figure 4.** *VIP preferentially activates caudal ARN kisspeptin neurons in female mice.* **A.**
43 Raw fluorescence traces from the rostral, middle and caudal aspects of the ARN from
44 503 the same diestrous female *Kiss1::GCaMP6f* mouse. The two-min 1 μ M VIP exposure
45 504 period is indicated by the grey bar and each colored line represents a different cell. **B.**
46 505 Higher resolution changes in fluorescence showing the response profiles of six caudal
47 506 kisspeptin neurons to VIP. **C.** Histogram showing the percentage of kisspeptin
48 507 neurons in the rostral, middle and caudal aspects of the ARN responding to VIP in
49 508
50
51
52
53
54
55
56
57
58
59
60

1
2
3 509 male and female mice (N=4 each) * $p < 0.05$ compared to all other groups, Two-way
4 510 ANOVA with *post-hoc* Tukey tests.

511

512 **Figure 5.** *AVP preferentially activates caudal ARN kisspeptin neurons in female mice.*

513 **A.** Raw fluorescence traces from the rostral, middle and caudal aspects of the ARN
514 from diestrous female *Kiss1::GCaMP6f* mouse. The two-min 300nM AVP exposure
515 period is indicated by the grey bar and each colored line represents a different cell.
516 Note the orange cell in the caudal traces that was discarded from analysis as it
517 exhibited a spontaneous fluctuation in fluorescence prior to the test with AVP. **B.**
518 Higher resolution change in fluorescence images showing the AVP response profiles
519 of five of the caudal kisspeptin neurons shown in A. **C.** Histogram showing the
520 percentage of kisspeptin neurons in the rostral, middle and caudal aspects of the ARN
521 responding to AVP in male and female mice (N=4 each). * $p < 0.05$ compared to all
522 other groups, Two-way ANOVA with *post-hoc* Tukey tests.

523

524 Table

	nos. Kiss neurons / hemi-section	% GCaMP6 cells +ve for kisspeptin	% kisspeptin cells +ve for GCaMP6
rostral ARN	37±14	88±7%	99±1%
middle ARN	60±7	94±1%	99±1%
caudal ARN	68±8	95±2%	99±1%

525

526 Table showing the numbers of kisspeptin-immunoreactive neurons detected in the
527 three subregions of the ARN and their levels of co-expression with GCaMP6. N = 4
528 ovariectomized female mice.

1
2
3
4
5
6
7
8
9
10
11
12
13
14
15
16
17
18
19
20
21
22
23
24
25
26
27
28
29
30
31
32
33
34
35
36
37
38
39
40
41
42
43
44
45
46
47
48
49
50
51
52
53
54
55
56
57
58
59
60

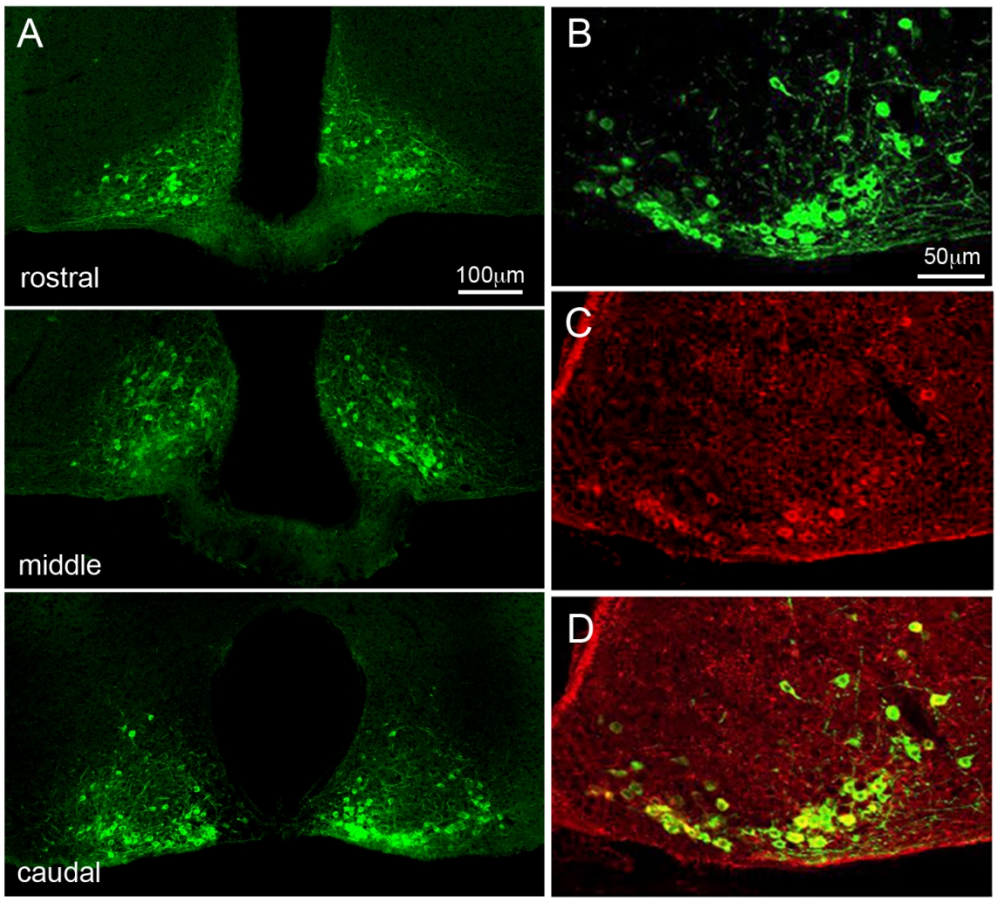


Figure 1.

Figure 1. Distribution of GCaMP6 in arcuate nucleus (ARN). A. Images from the same adult female mouse showing the GFP-immunofluorescence (GCaMP6) in the rostral, middle and caudal levels of the ARN. B-D, confocal images showing dual fluorescence for GFP- (B) and kisspeptin- (C) immunofluorescence, and with the overlapping signals represented in D.

123x122mm (300 x 300 DPI)

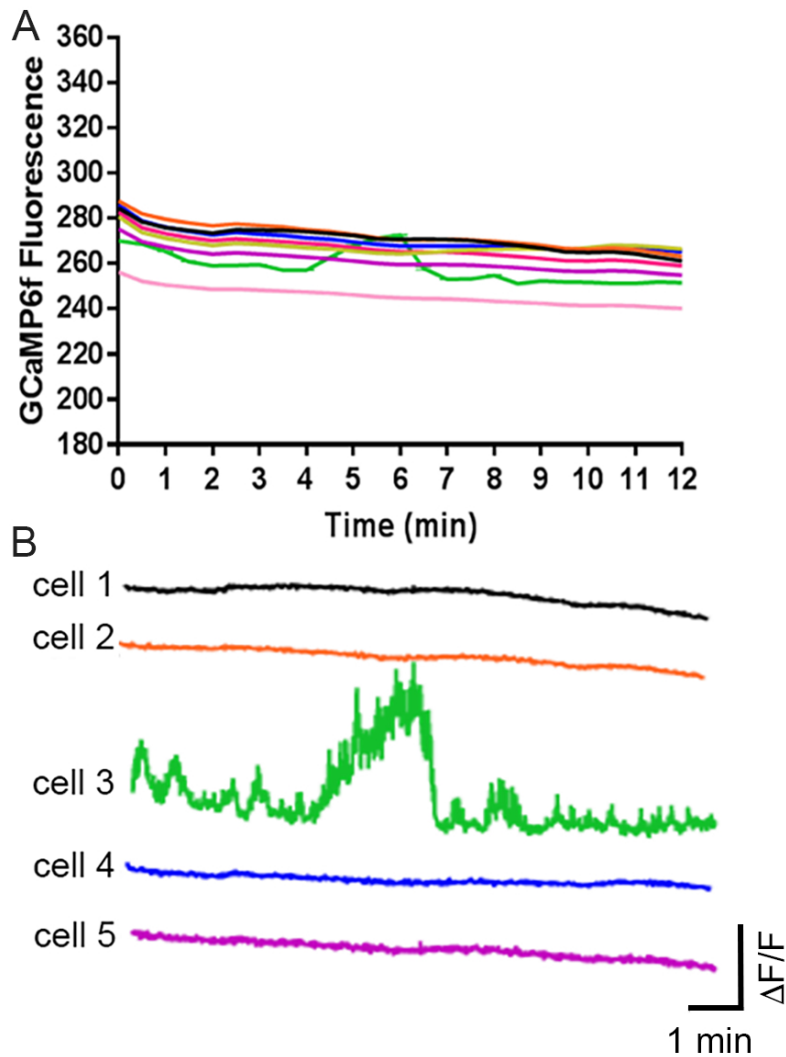


Figure 2

Figure 2. Baseline GCaMP6 fluorescence levels in arcuate kisspeptin neurons. A. Raw fluorescence levels of eight ARN kisspeptin neurons located in a middle arcuate nucleus brain slice over 12 min. B. Higher resolution change in fluorescence levels of 5 of these cells showing the one cell (cell 3) that exhibited spontaneous fluctuations.

76x110mm (300 x 300 DPI)

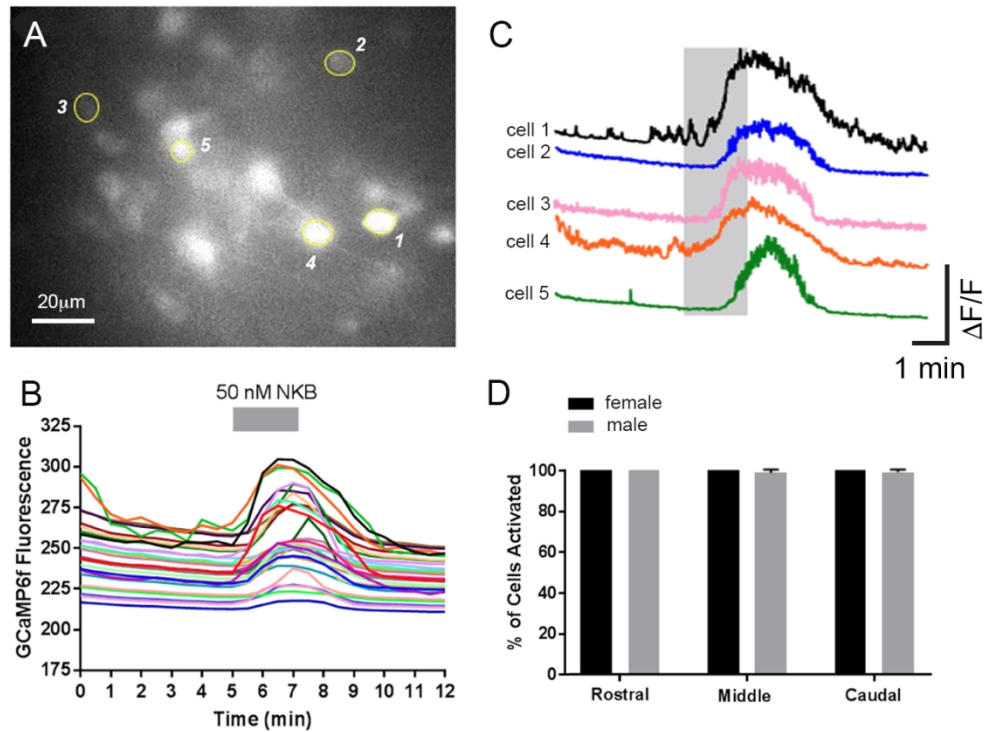


Figure 3

Figure 3. NKB activates essentially all kisspeptin neurons in both male and female mice. A. Single frame photograph of GCaMP6 fluorescence in the middle ARN of a slice being imaged. The five cells shown in C are labelled. B. Raw fluorescence recordings from 21 kisspeptin neurons in that brain slice showing their response to a 2-min application of 50nM NKB (grey bar) in the presence of TTX and amino acid receptor antagonists. C. Higher resolution change in fluorescence levels from the five cells depicted in A. Colors are the same as in B. D. Histogram showing the percentage of kisspeptin neurons in the rostral, middle and caudal aspects of the ARN that responded to NKB in male and female mice (N=4, each).

110x90mm (300 x 300 DPI)

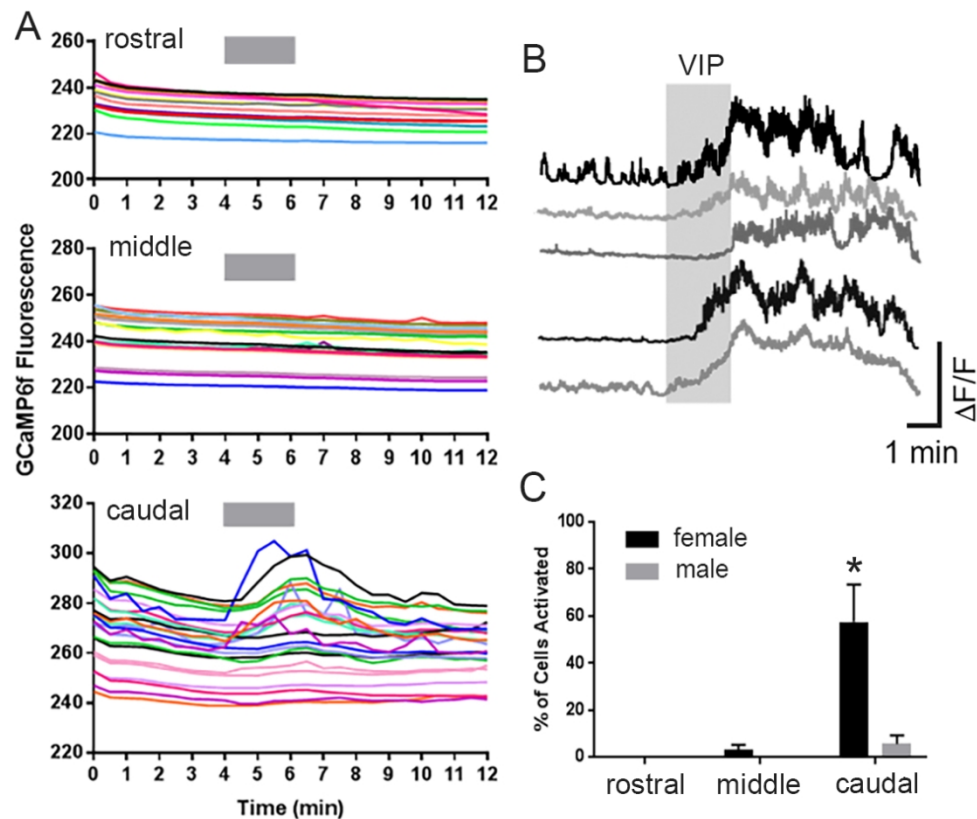


Figure 4

Figure 4. VIP preferentially activates caudal ARN kisspeptin neurons in female mice. A. Raw fluorescence traces from the rostral, middle and caudal aspects of the ARN from the same diestrous female Kiss1::GCaMP6f mouse. The two-min 1 μ M VIP exposure period is indicated by the grey bar and each colored line represents a different cell. B. Higher resolution changes in fluorescence showing the response profiles of six caudal kisspeptin neurons to VIP. C. Histogram showing the percentage of kisspeptin neurons in the rostral, middle and caudal aspects of the ARN responding to VIP in male and female mice (N=4 each) * $p < 0.05$ compared to all other groups, Two-way ANOVA with post-hoc Tukey tests.

98x90mm (300 x 300 DPI)

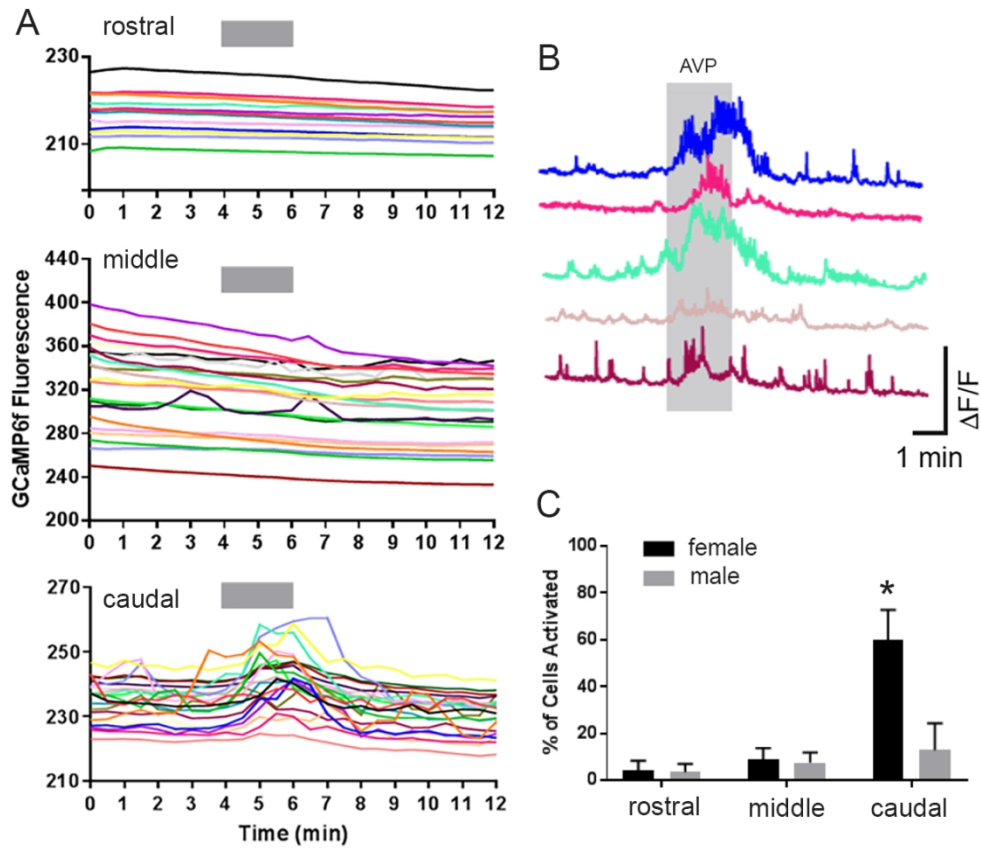


Figure 5

Figure 5. AVP preferentially activates caudal ARN kisspeptin neurons in female mice. A. Raw fluorescence traces from the rostral, middle and caudal aspects of the ARN from diestrous female Kiss1::GCaMP6f mouse. The two-min 300nM AVP exposure period is indicated by the grey bar and each colored line represents a different cell. Note the orange cell in the caudal traces that was discarded from analysis as it exhibited a spontaneous fluctuation in fluorescence prior to the test with AVP. B. Higher resolution change in fluorescence images showing the AVP response profiles of five of the caudal kisspeptin neurons shown in A. C. Histogram showing the percentage of kisspeptin neurons in the rostral, middle and caudal aspects of the ARN responding to AVP in male and female mice (N=4 each). * $p < 0.05$ compared to all other groups, Two-way ANOVA with post-hoc Tukey tests.

107x102mm (300 x 300 DPI)